BEHAVIORAL RESPONSE AND IMAGING OF MOTOR FLAGELLA IN *E. COLI*

An Undergraduate Research Scholars Thesis

by

LANDON CRISTIANO AZIZ

Submitted to the Undergraduate Research Scholars program
Texas A&M University
in partial fulfillment of the requirements for the designation as an

UNDERGRADUATE RESEARCH SCHOLAR

Approved by
Research Advisor: Dr. Michael Manson

May 2016

Major: Nuclear Engineering

TABLE OF CONTENTS

Page

ABSTRACT

Behavioral Response and Imaging of Motor Flagella in *E. Coli*

Landon Cristiano Aziz
Department of Nuclear Engineering
Texas A&M University

Research Advisor: Dr. Michael Manson
Department of Biology

Chemotaxis in *E. coli* is controlled by signaling from membrane-bound chemoreceptors to flagellar motors. This determines the direction that the flagella rotate. These flagellar motors can switch from clockwise (CW) to counter-clockwise (CCW) rotation in response to ligand binding to a chemoreceptor. The complete molecular mechanism of the switching process, however, remains to be explained. We will use mutant alleles of the serine chemoreceptor Tsr to probe the changes that take place in the flagellar motor during controlled switching from CW to CCW rotation, and vice versa, in *E. coli* mini-cells.

DEDICATION

I would like to dedicate this to my mother and God for always being consistent sources of motivation in pursuing better things for me in my life. I would not be able to accomplish as much as I have to this day without the strong foundation given to me by them and am eternally grateful for the positive influence they have had in my life thus far. In addition, my sister has always been supportive in me pursing my dreams as well, whether it be from encouraging me to do things outside my bubble or comforting me in my times of need she has been there with from the very beginning. At the end of the day, I would not be the person I am today without these important figures shaping who I am.

ACKNOWLEDGMENTS

I would like to acknowledge Dr. Michael Manson who let me take his introductory biology course even though I was not a biology major and then let me join his lab when I took an interest in research giving me the opportunity to broaden my knowledge in the field of biology past just introductory biology. In addition to Dr. Manson, Dr. Louis Morgan directly supervised my project and guided me when I had any questions about results and interpreting them in a scientific manner. Lastly, Rachel Wright was a tremendous help and mentored me when I first joined the Manson lab. She gave me a solid foundation in learning the major experiments run in the lab and giving me the tools to become a well-rounded researcher.

NOMENCLATURE

MCPs- methyl-accepting chemotaxis proteins

Tsr- taxis towards serine, away from leucine, indole and weak acids

CW- clockwise

CCW- counter clockwise

GFP- green fluorescent protein

IPTG- isopropyl-beta-D-thiogalactopyranoside

CHAPTER I

INTRODUCTION

The *E. coli* chemotaxis system is a prototypical model for studying signal transduction. Membrane-bound MCPs (methyl-accepting chemotaxis proteins) transduce signals to control flagellar rotation. MCPs are arranged in chemoreceptor complexes that interact with the CheA/CheW protein complex, which transmits signals from the MCPs to the flagella by a phosphor-relay pathway (1).

In the absence of a ligand binding to a chemoreceptor, the CheA histidine kinase phosphorylates CheY, which allows it to bind to flagellar motors and cause them to rotate in a CW direction. This results in tumbling behavior for the bacteria. When a MCP binds a signal ligand the kinase activity of CheA is blocked, CheY becomes dephosphorylated by CheZ, and the flagella rotate in a CCW direction. This results in a smooth swimming behavior. In addition, CheR and CheB methylate or demethylate, respectively, MCP residues to reduce their signal threshold sensitivity; this ensures cells will swim up a gradient of an attractant chemical. CheB, like CheY, is also a target for CheA phosphorylation (1).

The serine-sensing Tsr chemoreceptor is one of the most abundant MCPs and its structure has been well studied biochemically and genetically (2). Mutational analysis has revealed mutant alleles of the Tsr chemoreceptor that lock the CheA into “kinase on” or “kinase off” signaling states (3). These two states cause the flagella to rotate exclusively in either CW (on) or CCW (off) directions. The CW and CCW rotational directions have been confirmed by both the

tethered cell assay—fluorescent labelling of cells with GFP when flagella are bound to a glass slide using anti-flagellar antibodies, and recording which direction the cells spin—and by directly staining the flagella with Oregon Green and imaging under a fluorescent microscope (4).

E. coli "skinny mini-cells" carry *ΔminCDE* and *mreB-A125V* mutations that result in small, round, DNA-less cells that are ideal for imaging studies. Previously skinny mini-cell strains have been used to generate 3-D cryoelectron tomography images of chemoreceptor arrays (5). This project is part of a larger project designed to capture 3-D images of the Tsr chemoreceptor and the flagella motors when each are in a known structural/signaling state.

The samples UU2766, which has CheB present, and UU2768, which has CheR expressed, were acquired from Dr. John Parkinson of the University of Utah at Salt Lake City. The cells have deleted Tsr chemoreceptors on their chromosomes, but obtain these chemoreceptors from the plasmids pRR53 Tsr-A413G and pRR53 Tsr-A413V creating four samples: UU2766 A413G, UU2768 A413G, UU2766 A413V, and UU2768 A413V. The chemoreceptors CheR and CheB are both required for adaptation in the cells and in the absence of one or both no chemotactic adaptation occurs. The cells stay in one signaling state and do not revert back when no adaptation occurs.

CHAPTER II

METHODS

Strains are available that lack all five MCP-encoding genes (*Δtar, Δtsr, Δtap, Δrgb, Δaer-1*), allowing for the study of single-receptor cells by using a plasmid-carried copy of a gene under a controllable promoter (3). We will transform plasmids into *E. coli* skinny mini-cells that express various *tsr* alleles from the IPTG-inducible *lac* promoter, and are capable of locking the chemotaxis system in "kinase on" or "kinase off" states.

These mini-cells also lack the genes responsible for adaptation of the chemotaxis system (*ΔcheR, ΔcheB*). This allows us to switch the signaling state of the "locked" Tsr receptors, using attractant or repellant chemoeffectors appropriately, into the opposite signaling state and observe swimming behavior of the cells without the chemotaxis adaptation system causing the behavior to revert to unstimulated behavior. The Tsr mutations occur at the 413 residue of the Tsr cytoplasmic tail that interacts with the CheA/CheW complex. In normal *E. coli* cells, the A413V mutation results in a kinase-off signaling state and smooth swimming behavior; conversely, the A413G mutation results in constant tumbling behavior (3, 6).

The swimming behavior of skinny mini-cells expressing these alleles will be characterized using phase-contrast microscopy and GFP fluorescent microscopy. Flagellar will be stained with Oregon Green and imaged on an epifluorescent microscope. Tethered mini-cell assays will be performed on an Olympus phase-contrast microscope. In each case, short videos will be produced using a CCD camera controlled by either the Olympus Micro DPController or

SimplePCI (Legacy) programs. Analysis of videos, and still images extracted from the videos, will be performed using ImageJ, a public-access program developed at the NIH.

The ImageJ program allows for the analysis of the UU2766 A413G, UU2768 A413G, UU2766 A413V, and UU2768 A413V bacteria samples. Each sample is divided into two subgroups, so in total eight subgroups are obtained. The first subgroup of each bacteria sample lacks the amino acid serine while the second subgroup contains a specific volume of serine. Videos of the bacteria's behavior are recorded of the top layer and bottom layer of the slide checking for consistency in motion of the bacteria. Using ImageJ frame-by-frame tracking of the bacterial movement is acquired. Further analyzing the tracking a three dimensional projection of the bacteria's movement can be formed which allows for numerical quantification of cellular motility such as displacement, distance traveled, speed, and direction. These values help determine the effect of a specific volume of serine has on the chemoreceptors of the bacteria.

CHAPTER III

RESULTS

Analyzing the UU2766 413G, UU2768 413G, UU2766 413V, and UU2768 413V samples using the ImageJ application, several differences between each sample were observed and recorded. Tracking UU2766 413G, which is a strain that has CheB expressed, showed little distinct motility without serine in the sample population observed which indicates a normal Brownian motion response. In the presence of 1 µM serine, no major behavioral response change was noted, indicating that UU2766 413G results in random unbiased motion regardless of serine present or not. The lack of significant motor function signifies the unsuccessful engaging of the kinase locking mechanism to induce swimming motion as opposed to tumbling or counterclockwise motion to clockwise motion from bottom to top of the slide. Figures 5 through 16 highlight the tracking of UU2766 413G cell sample.

UU2766 413V tracking resulted in a sizeable population sample observed. The sample tumbled in a normal random motion and in the addition of serine the motility significantly changed to swimming smoothly. The kinase mechanism complex was successfully locked and unlocked as the motion switched from counterclockwise to clockwise motion from the bottom of the slide to the top. In Figure's 1 through 4 the sample UU2766 413V was video recorded to highlight the tracking the cell movement, creating a path tracking image and an image that numbered each mini cell that was tracked. After adding serine to the cells the major distinction within the sample was the physical response the flagella had to the serine. At the bottom of the slide the cells travelled in a counter-clockwise manner, this is highlighted by the red circle place on 27 in

Figure 1 and in Figure 2. However, by the time the cells were monitored at the top of the slide the cells were observed to be traveling in a clockwise movement this is highlighted by the blue circle in Figure's 3 and 4. The importance of these two observations is also that the paths are relatively smooth meaning that the mini cell did not deviate from its curving path, if the paths were more jagged in nature, more Brownian motion then the cell would be considered to have been tumbling. The clockwise flagella rotation indicates that the kinase mechanism was shifted on and when the cells reversed to counterclockwise motion the kinase complex was shifted to the off phase.

UU2768 413G sample with CheR being expressed instead of CheB, the signaling state change and how the cells adaptation response was affected producing inconsistent data. Without serine introduced to the cells at the bottom of the slide traveled both Brownian motion and distinct biased motion. The cells tumbled in a clockwise and counterclockwise motion rather tumbling without distinct motion or swimming in a rather straight line. However, moving the microscope to image a different part of the bottom of the slide and tracking the cells resulted in smooth swimming motion and mixed arced motion. When serine was implemented adding a concentration gradient the cells that were smooth swimming and traveling in a circular path began traveling randomly, increasing tumbling at the bottom of the slide. At the top of the slide the cells had increased tumbling motion but still had distinct straight line swimming as well as arced motion. Refer to figures 25 to 31 for the described motion.

UU2768 413V sample also has CheB deleted while expressing CheR had ample Brownian motion with just a few cells swimming relatively straight both at the top of the slide and at the

bottom of the slide. In the presence of serine any apparent swimming was observed previously was gone. The entire slide had increased motility traveling greater distance in the same amount of time but tumbling a greater amount.

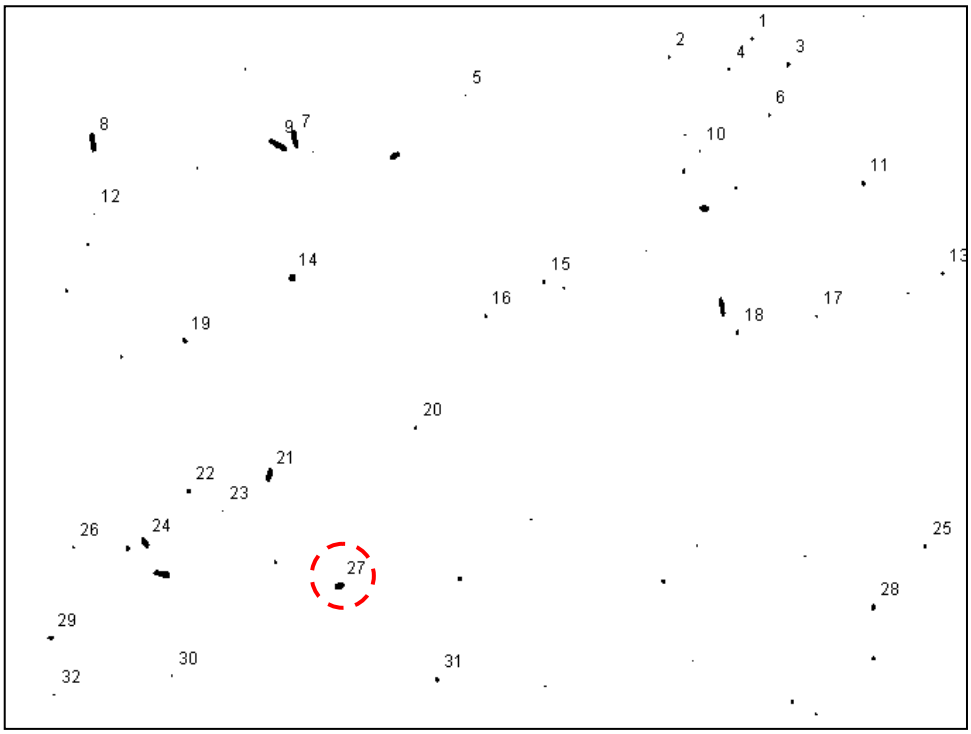

Figure 1. UU2766 413V, serine added, bottom of slide with numbered labels

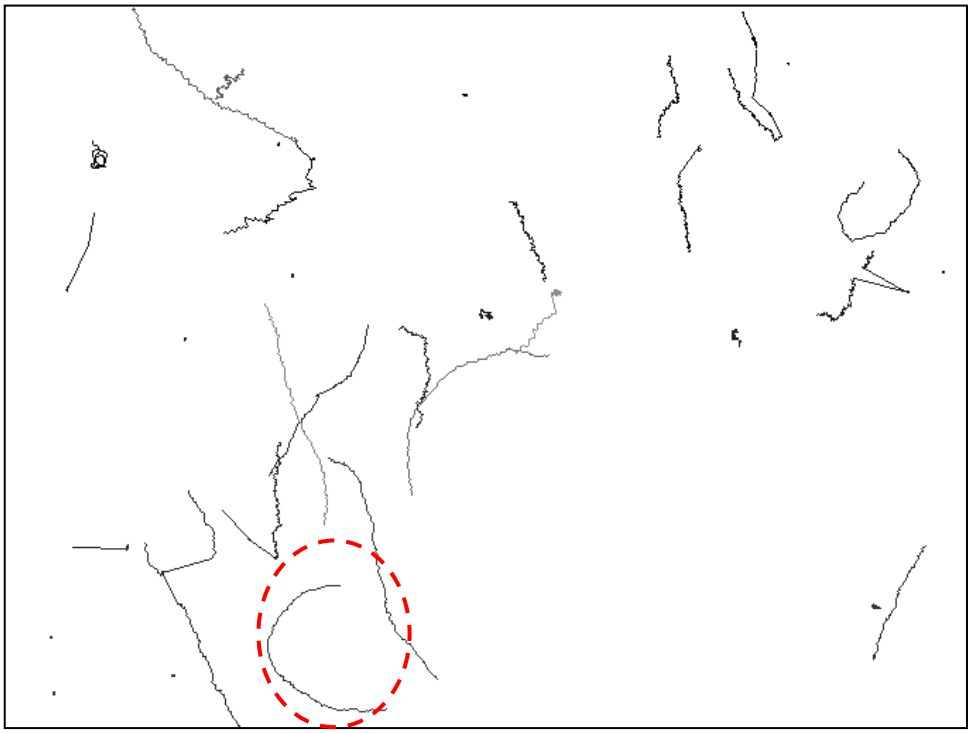

Figure 2. UU2766 413V, serine added, bottom of slide with numbered paths

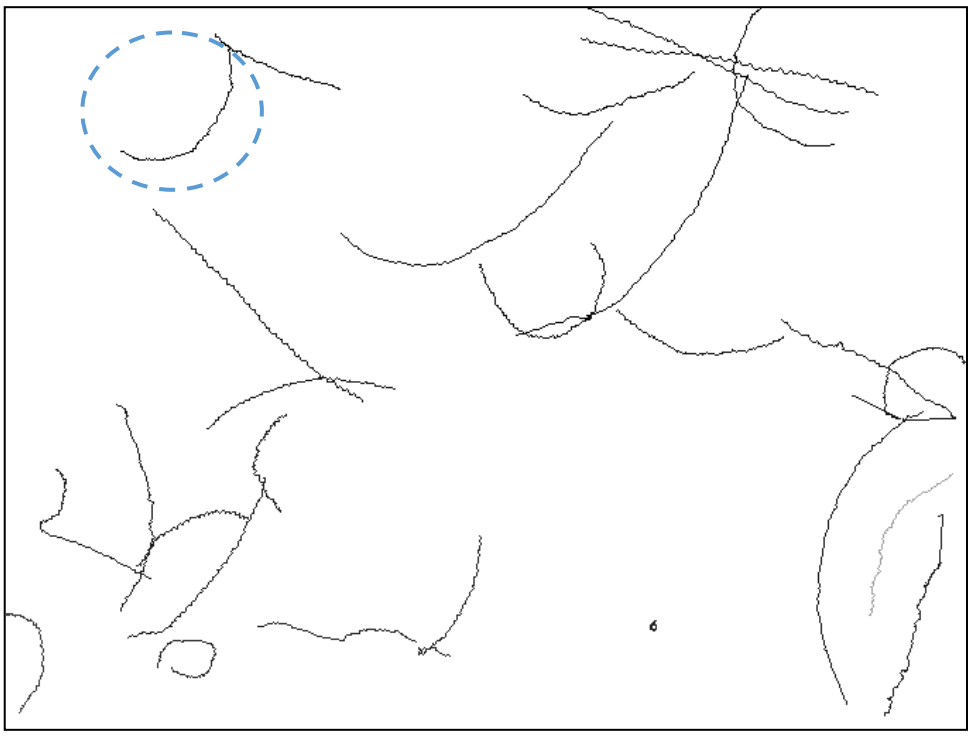

Figure 3. UU2766 413V, serine added, top of slide with paths

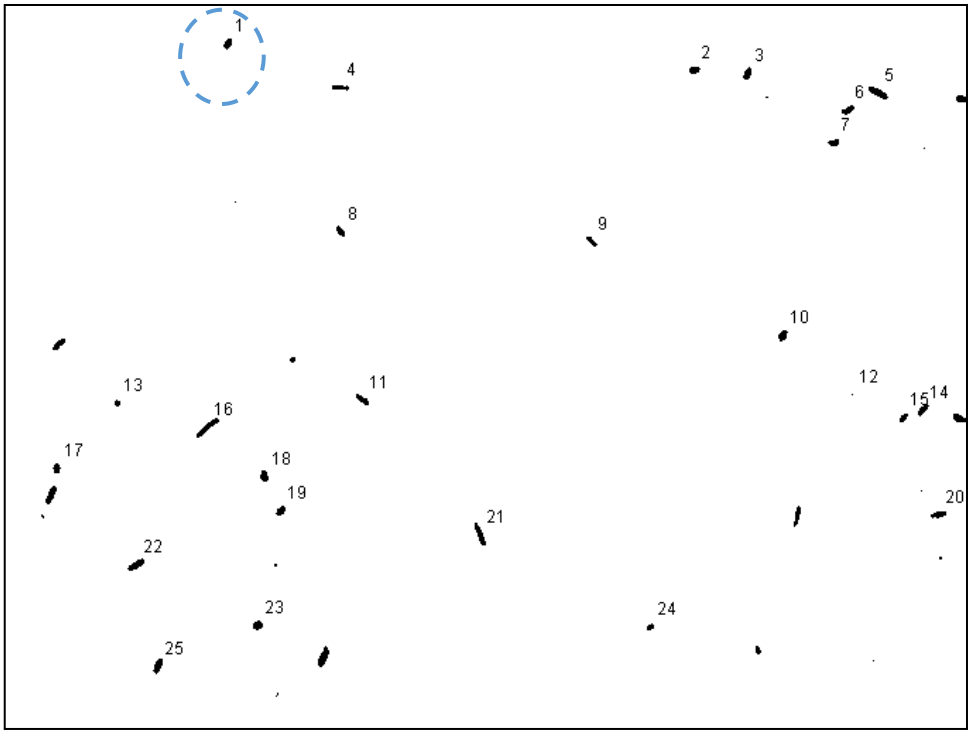

Figure 4. UU2766 413V, serine added, top of slide with numbered labels

UU2766 413G

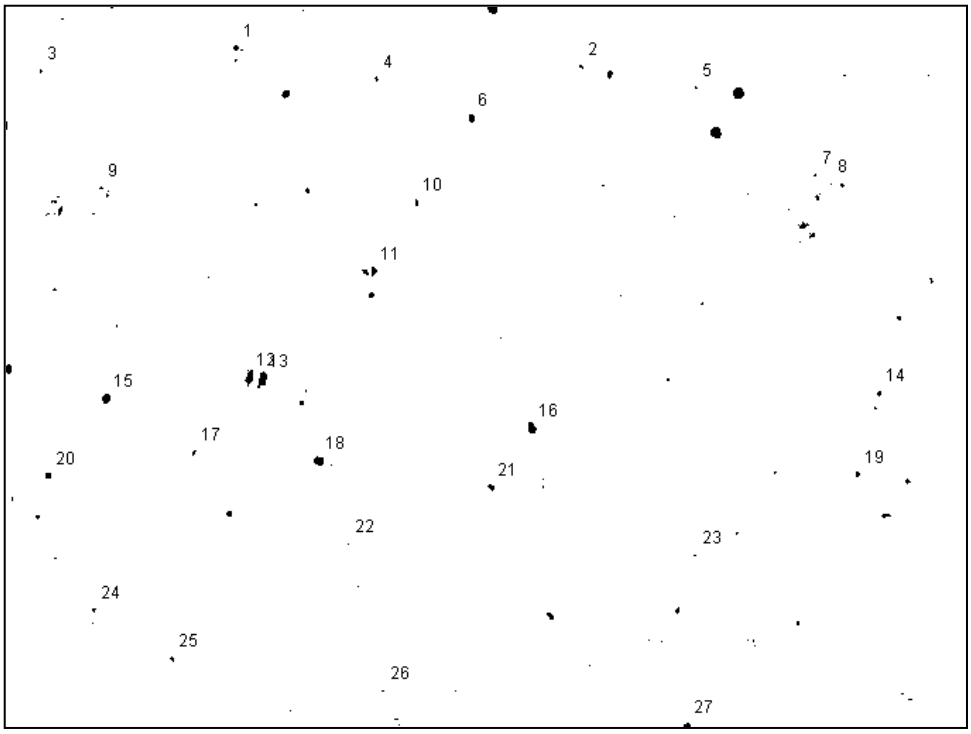

Figure 5. UU2766 413G, no serine, first bottom of slide with numbered labels

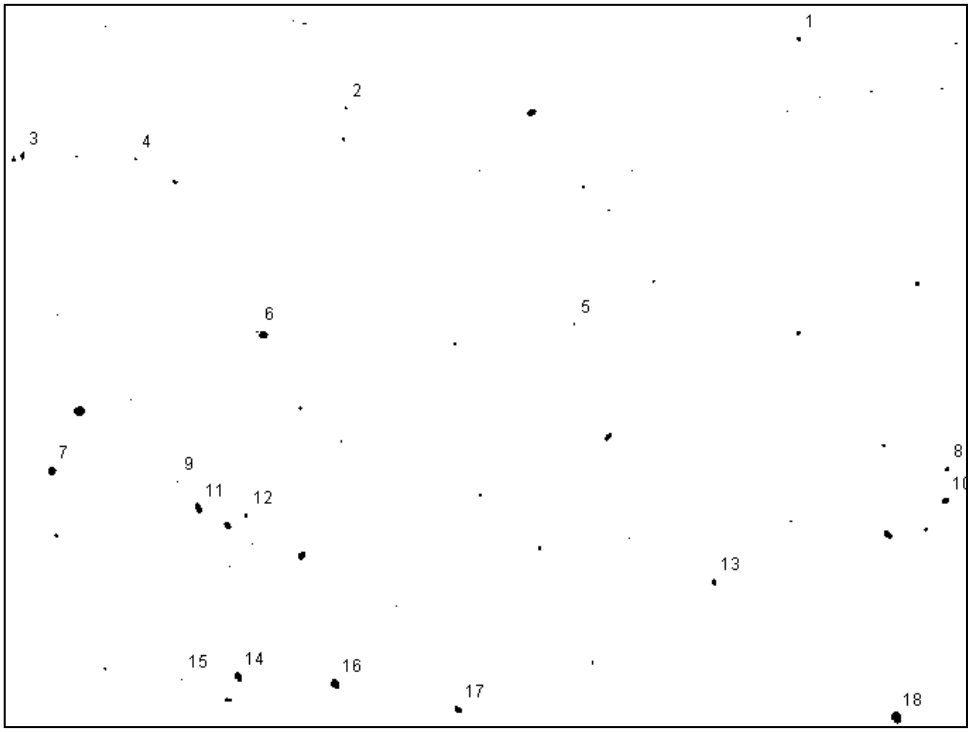

Figure 6. UU2766 413G, no serine, second bottom of slide with numbered labels

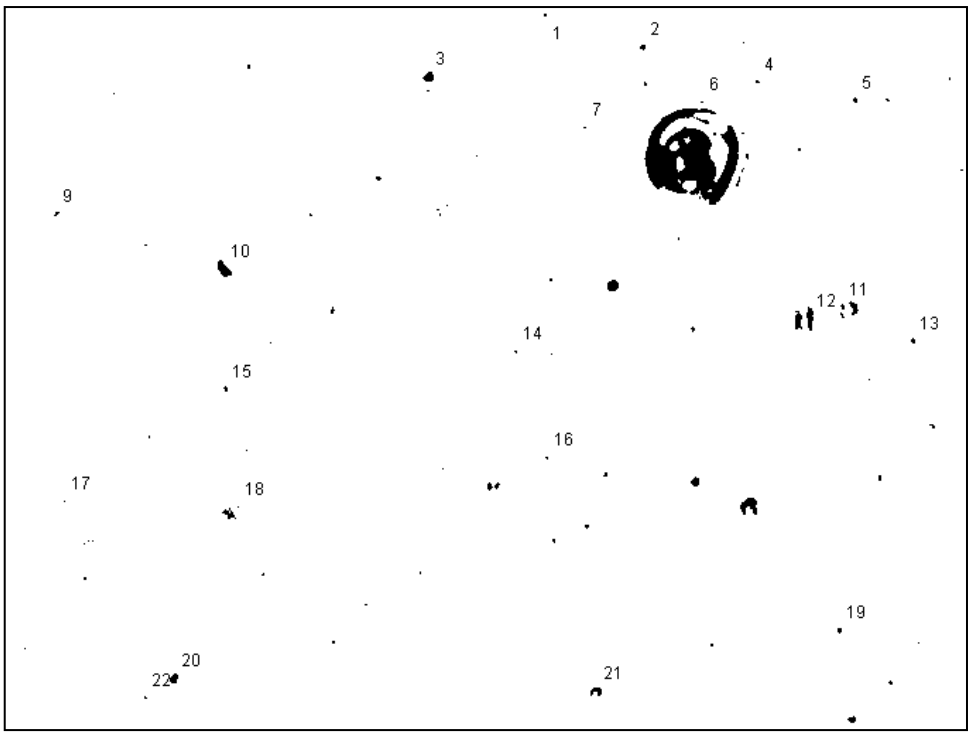

Figure 7. UU2766 413G, no serine, third bottom of slide with numbered labels

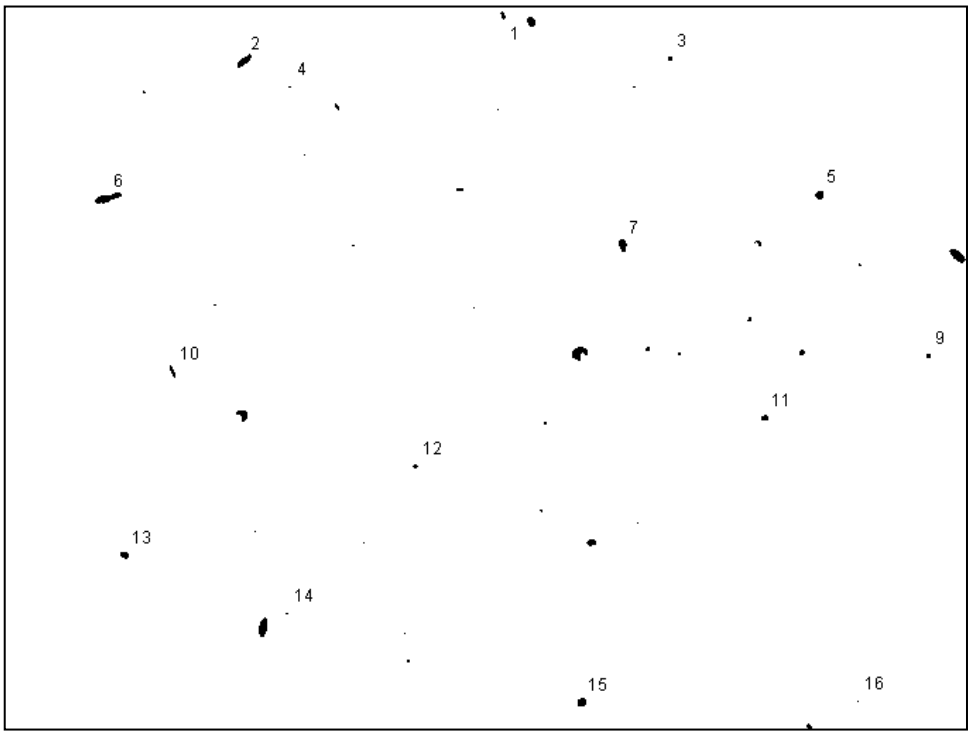

Figure 8. UU2766 413G, no serine, fourth bottom of slide with numbered labels

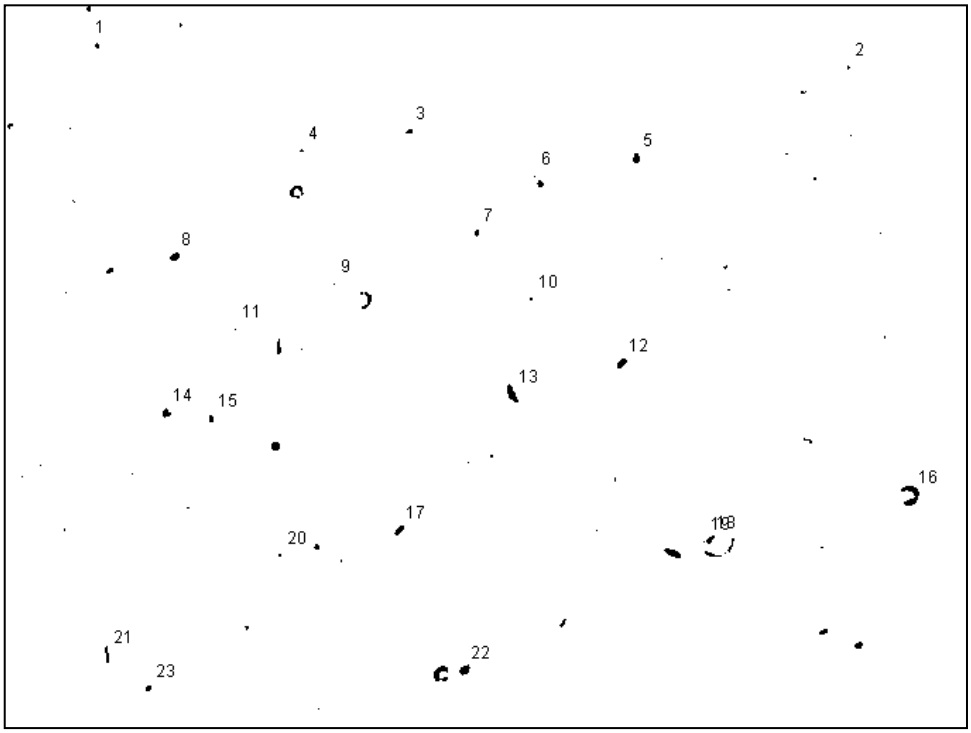

Figure 9. UU2766 413G, no serine, top of slide with numbered labels

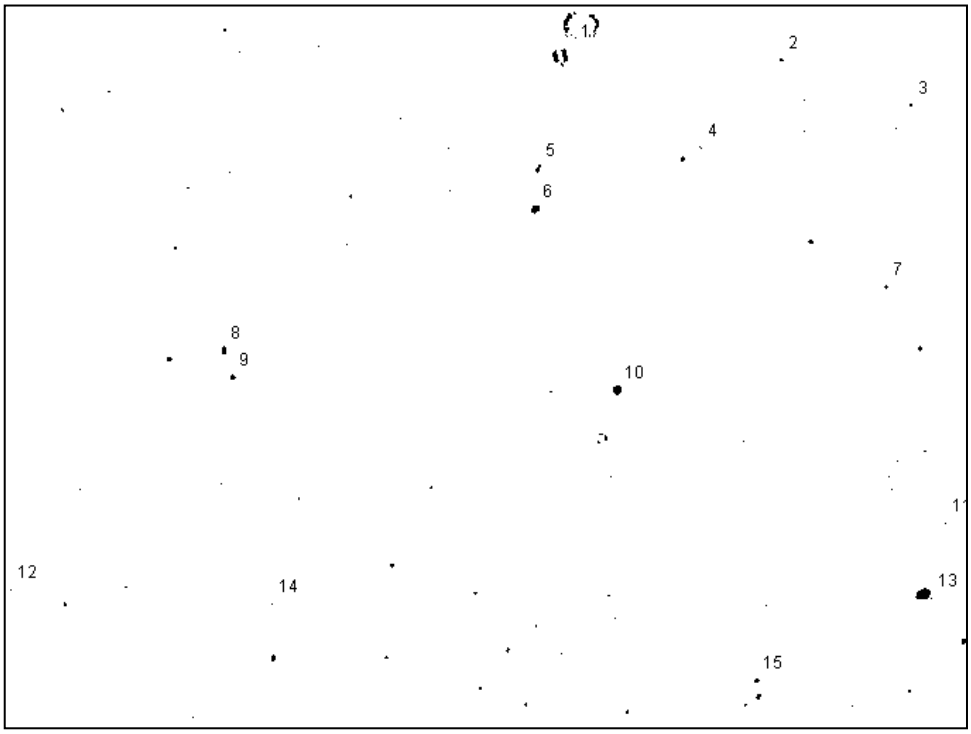

Figure 10. UU2766 413G, 1µM serine added, top of slide with numbered labels

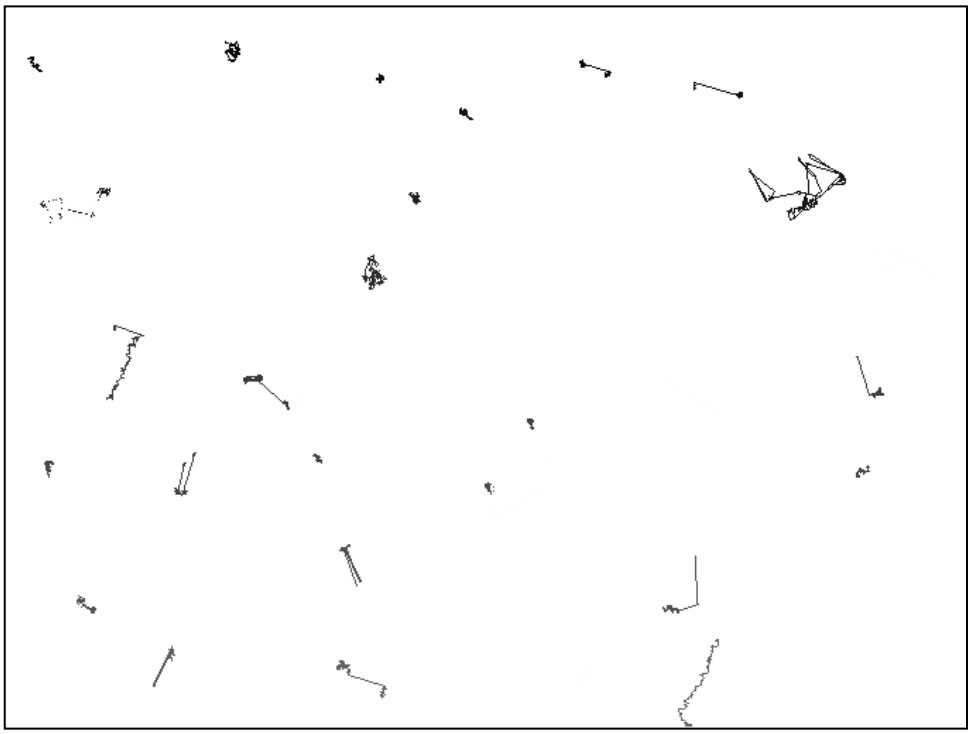

Figure 11. UU2766 413G, no serine added, first bottom of slide with tracked paths

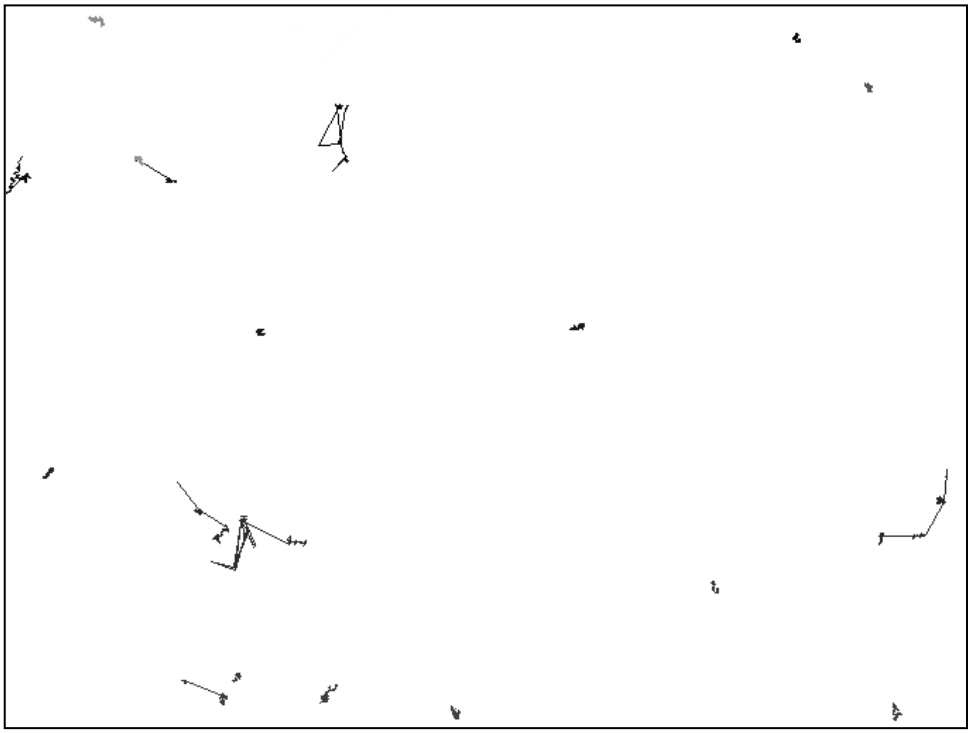

Figure 12. UU2766 413G, no serine added, second bottom of slide with tracked paths

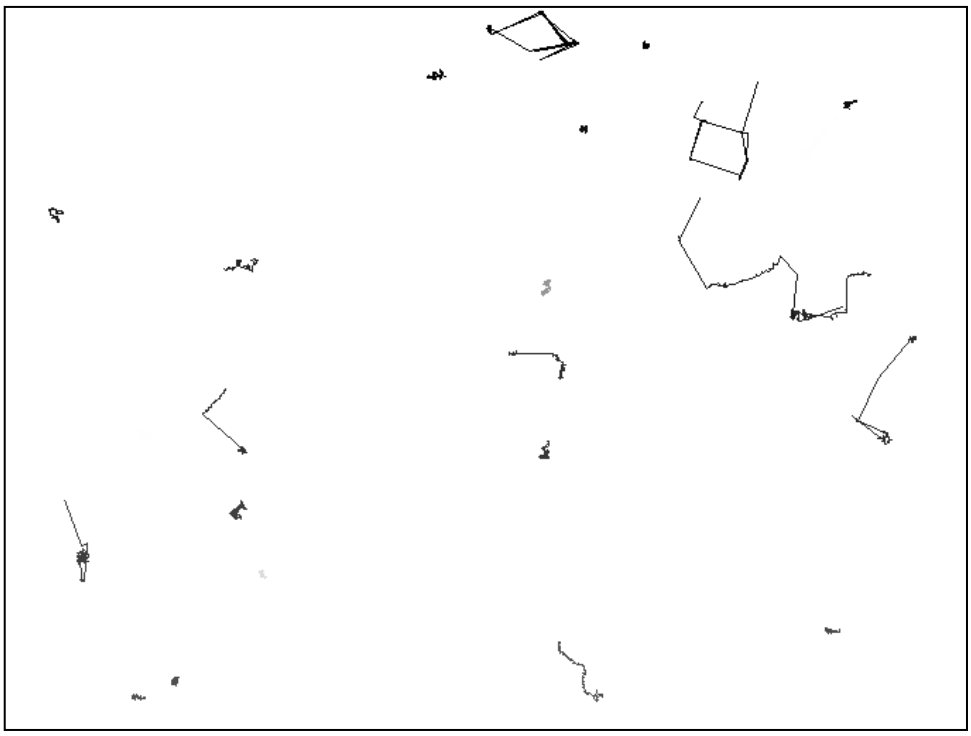

Figure 13. UU2766 413G, no serine added, third bottom of slide with tracked paths

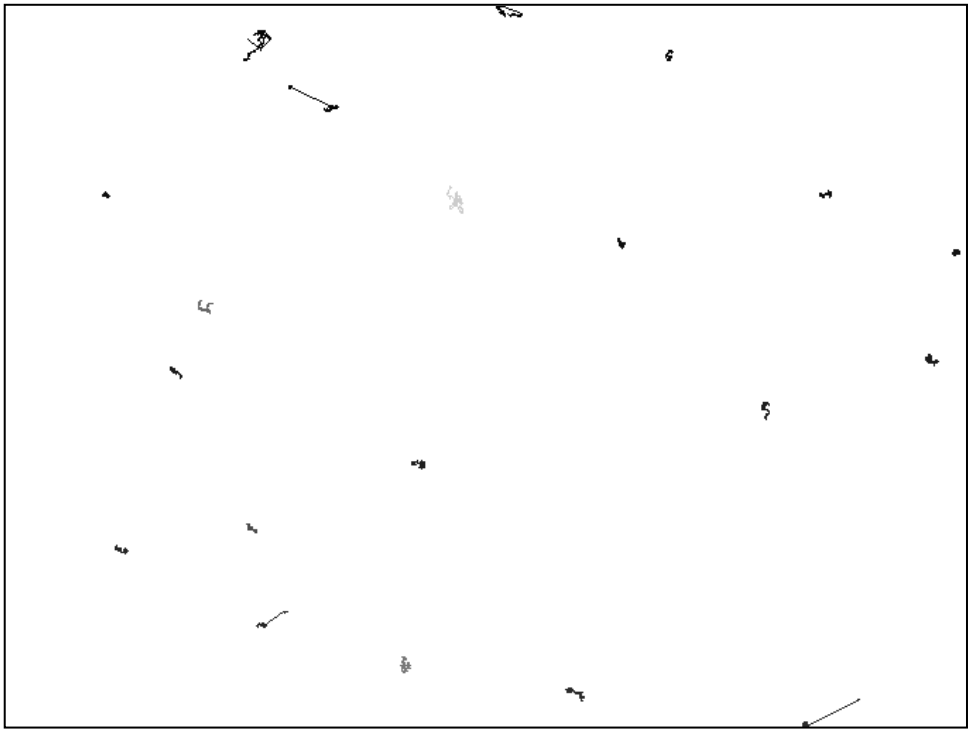

Figure 14. UU2766 413G, no serine added, fourth bottom of slide with tracked paths

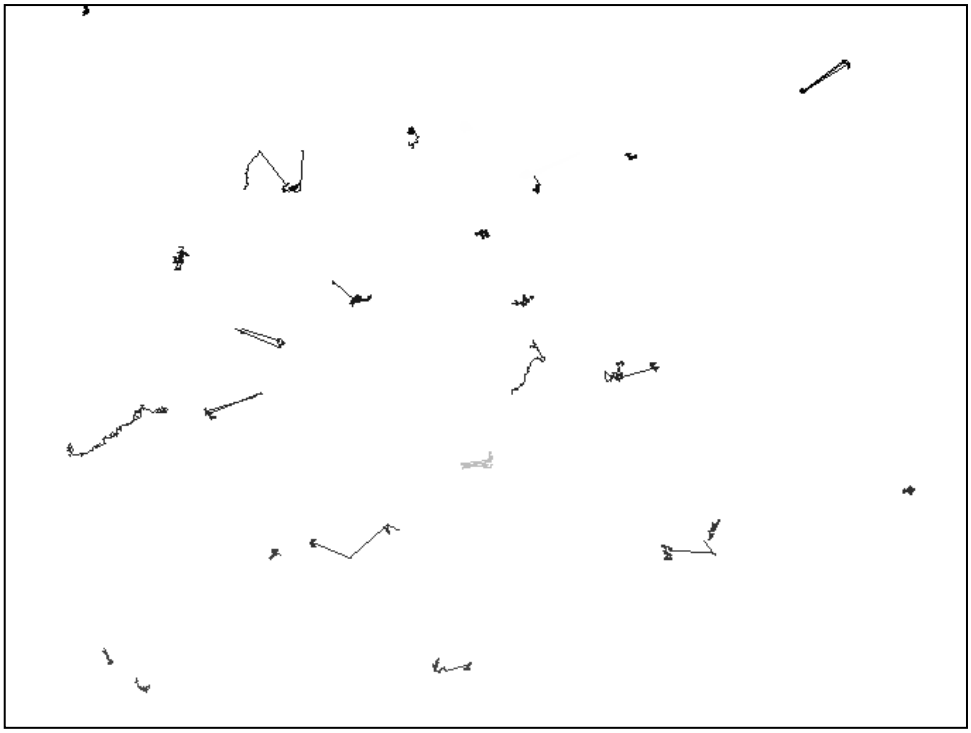

Figure 15. UU2766 413G, no serine added, top of slide with tracked paths

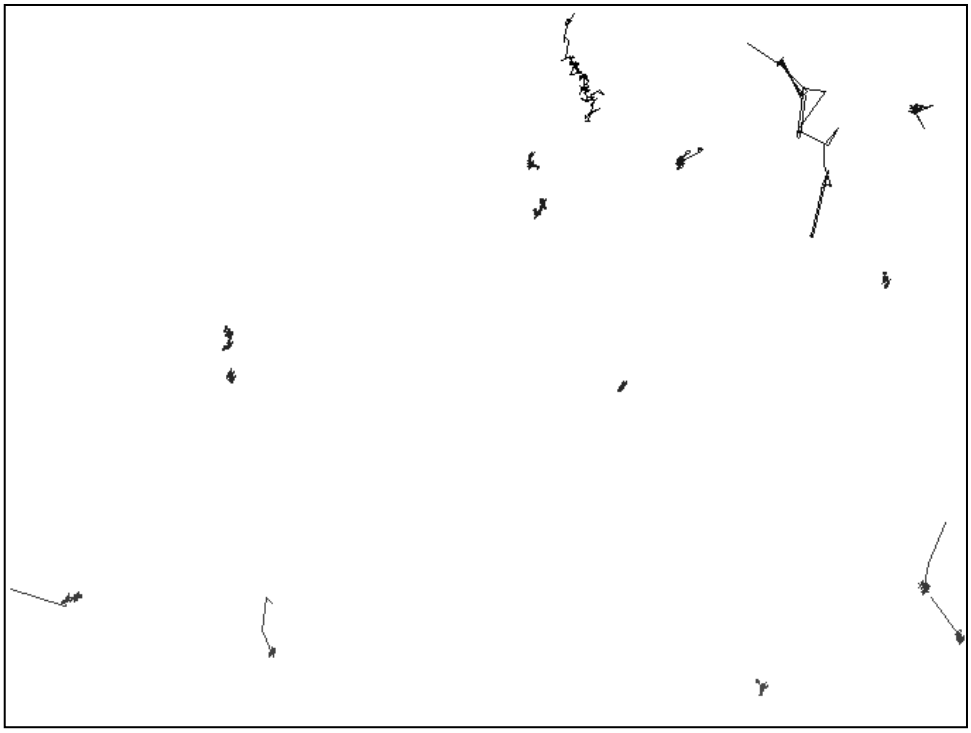

Figure 16. UU2766 413G, 1µM serine added, top of slide with tracked paths

UU2766 413V

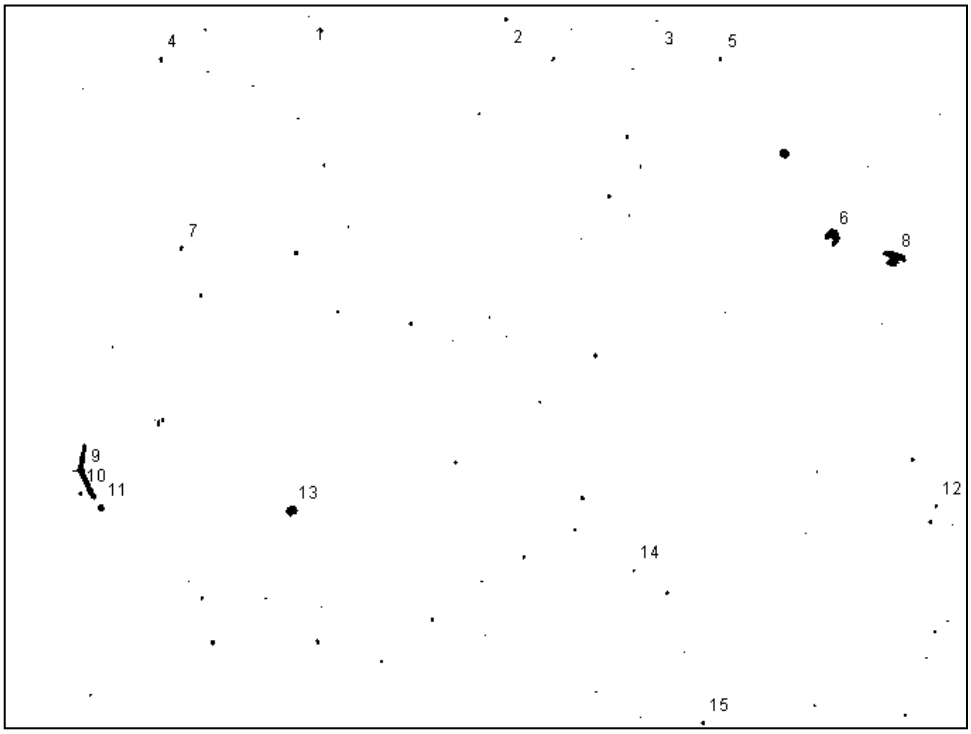

Figure 17. UU2766 413V, no serine, bottom of slide with numbered labels

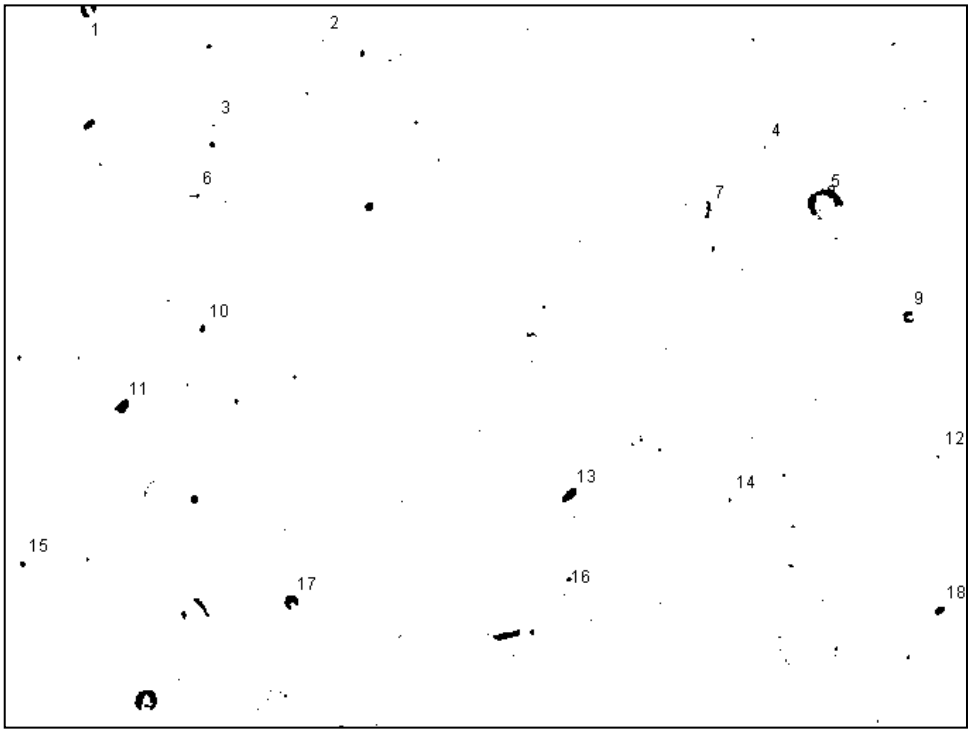

Figure 18. UU2766 413V, no serine, top of slide with numbered label

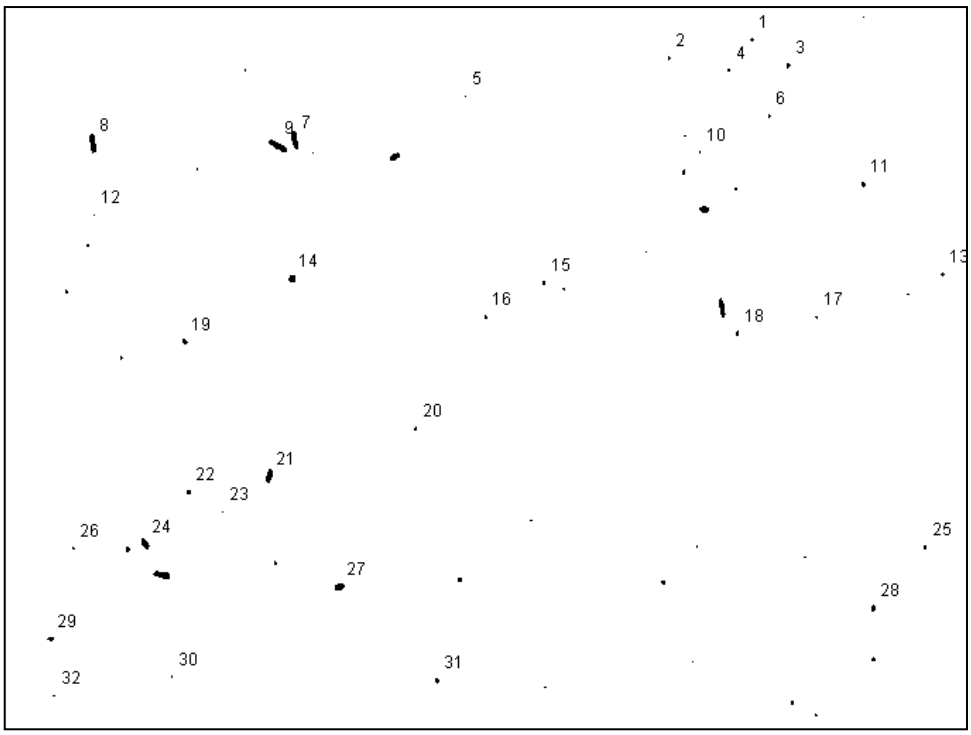

Figure 19. UU2766 413V, 1µM serine added, bottom of slide with numbered labels

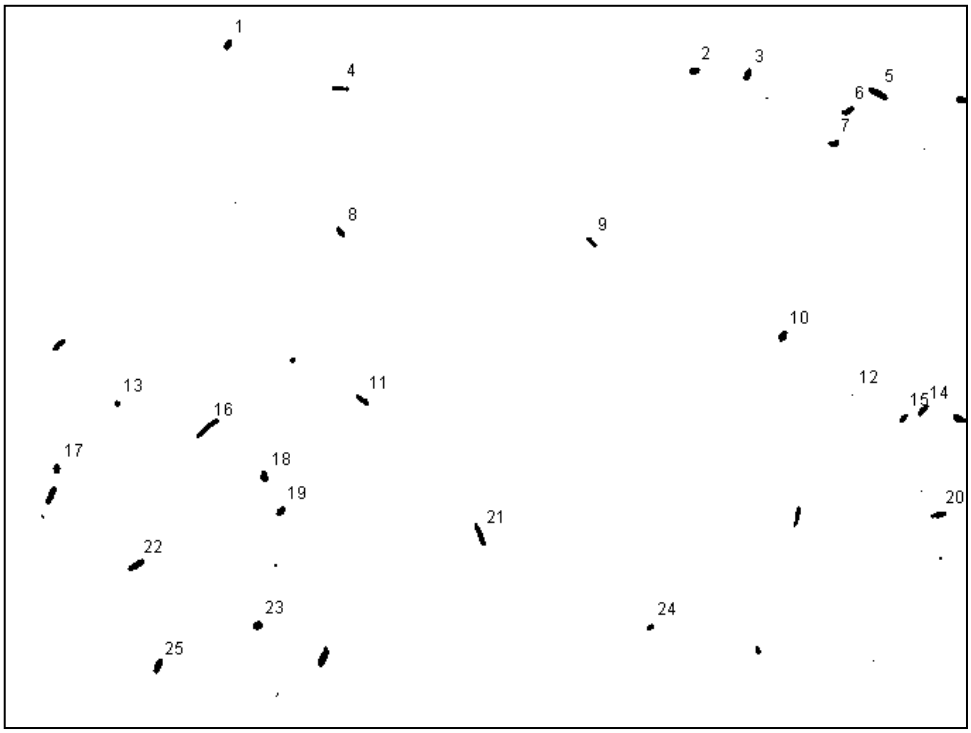

Figure 20. UU2766 413V, 1 µM serine added, top of slide with numbered labels

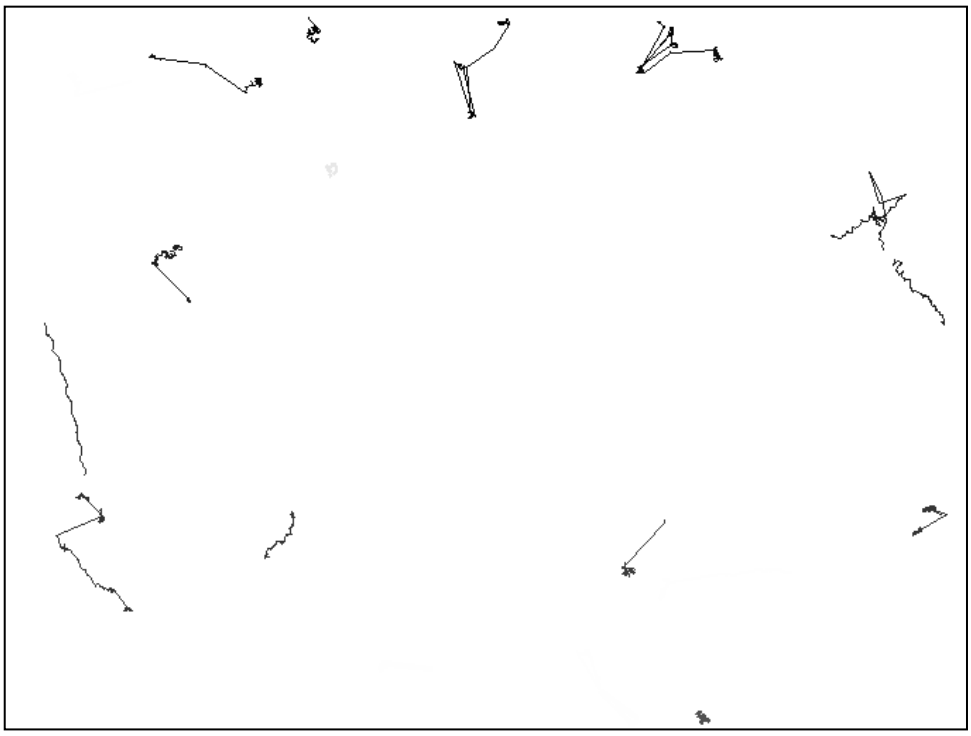

Figure 21. UU2766 413V, no serine added, bottom of slide with tracked paths

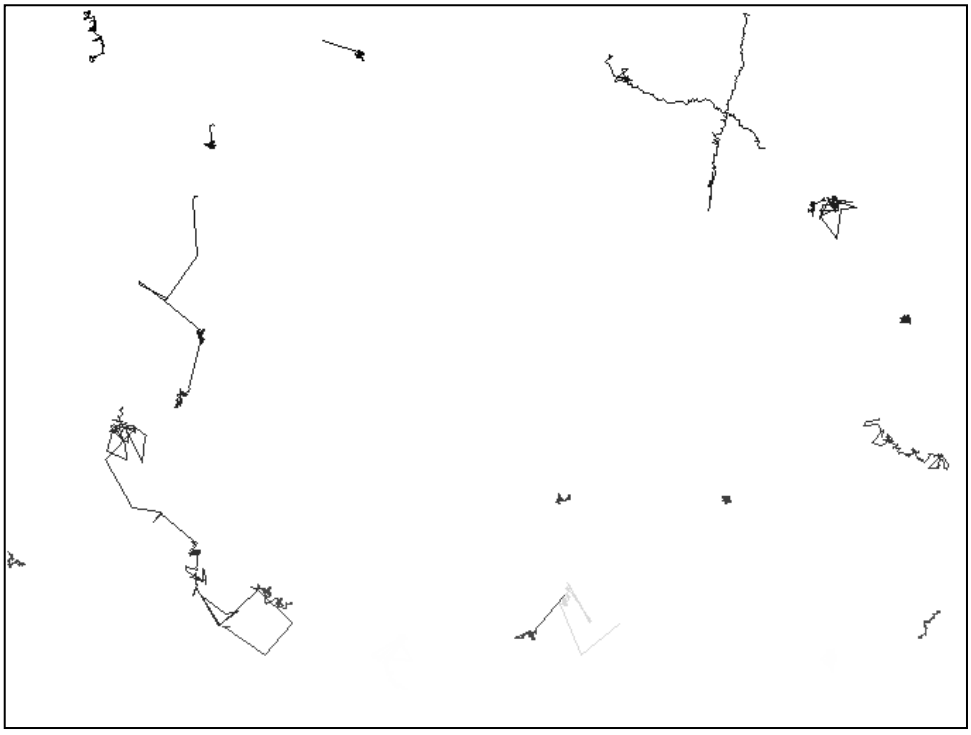

Figure 22. UU2766 413V, no serine added, top of slide with tracked paths

Figure 23. UU2766 413V, 1µM serine added, bottom of slide with tracked paths

Figure 24. UU2766 413V, 1 µM serine added, top of slide with tracked paths

UU2768 413G

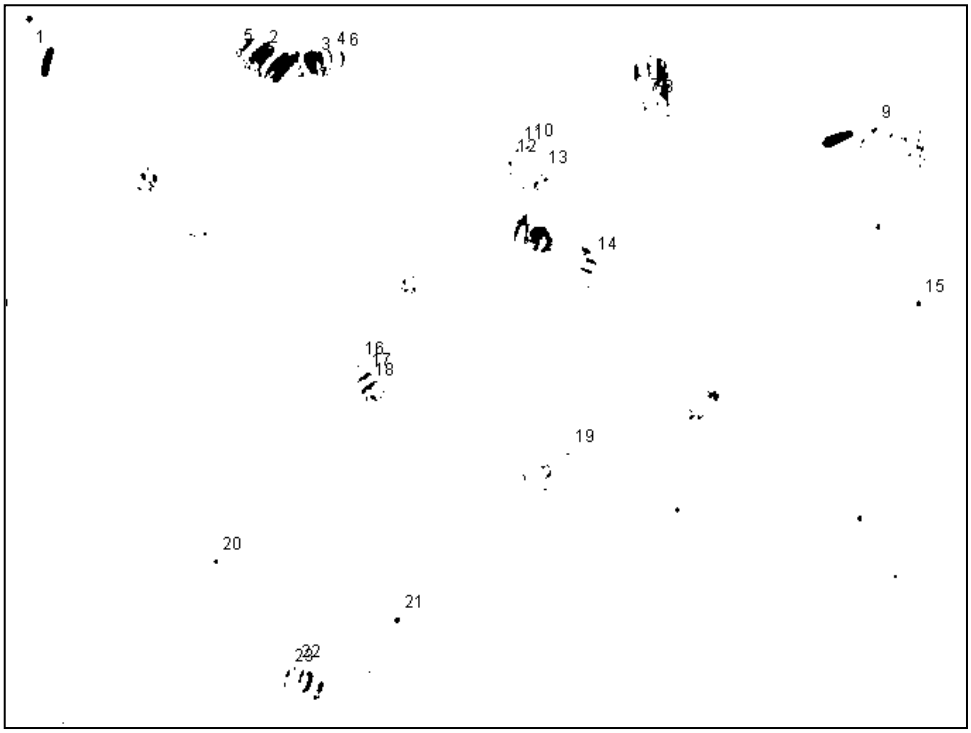

Figure 25. UU2768 413G, no serine, bottom of slide with numbered labels

Figure 26. UU2768 413G, no serine, second bottom of slide with numbered labels

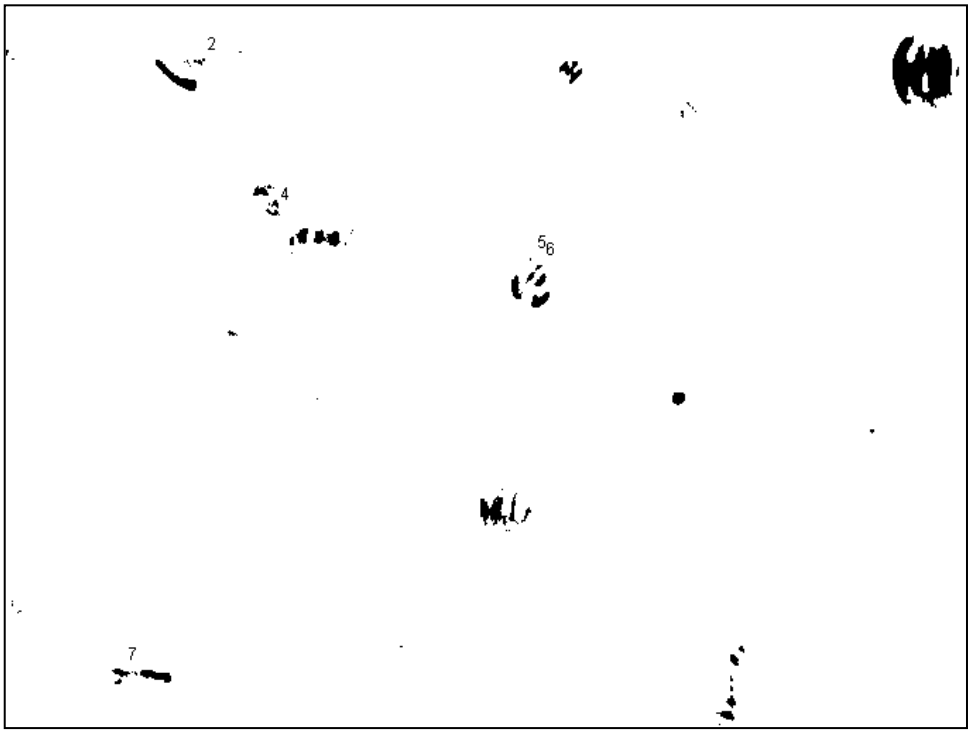

Figure 27. UU2768 413G, 1 µM serine added, bottom of slide with numbered labels

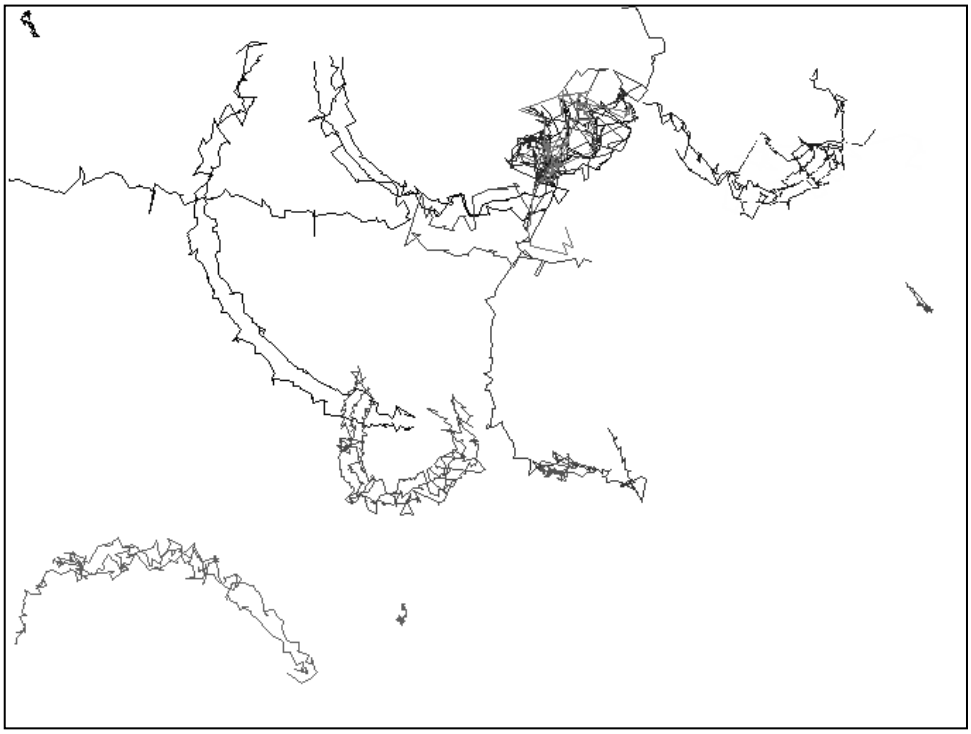

Figure 28. UU2768 413G, no serine added, bottom of slide with tracked paths

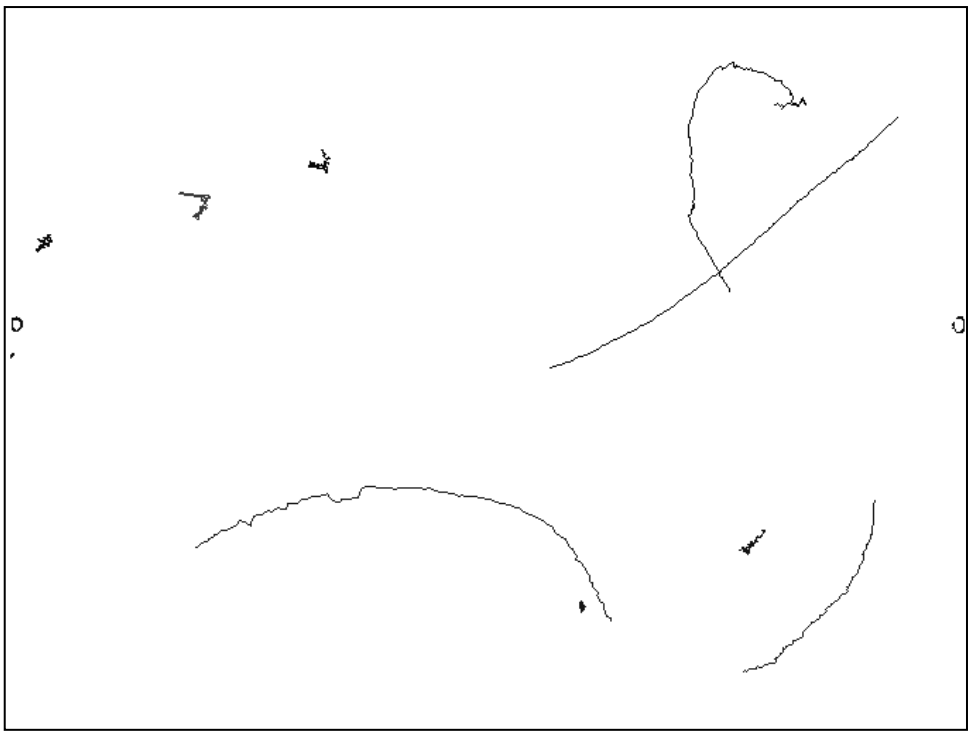

Figure 29. UU2768 413G, no serine added, second bottom of slide with tracked paths

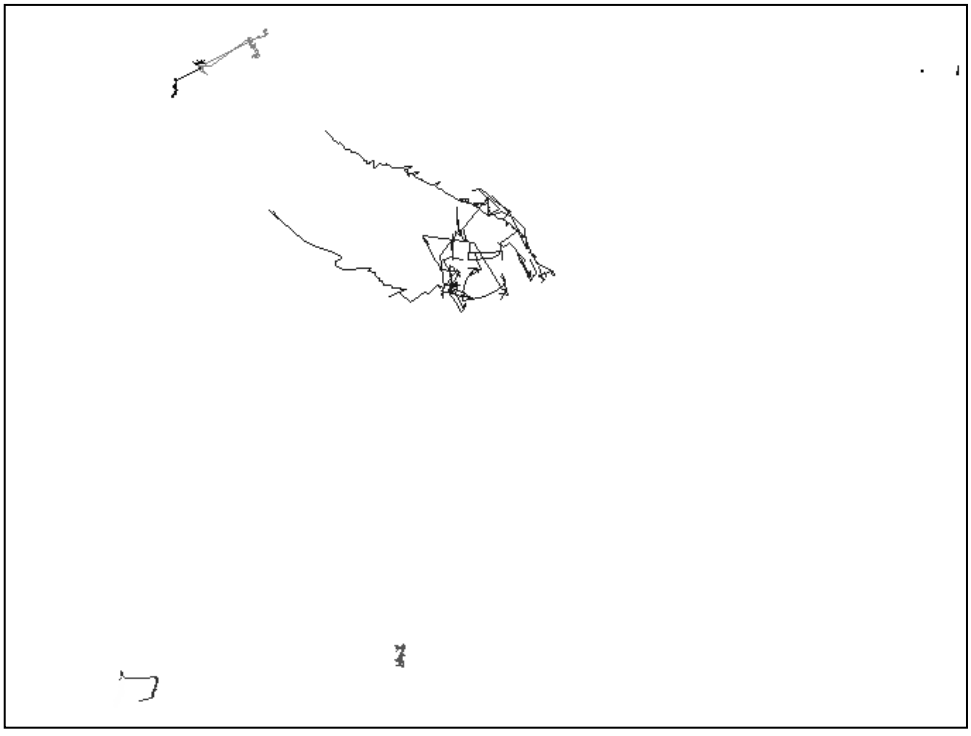

Figure 30. UU2768 413G, 1 μM serine added, bottom of slide with tracked paths

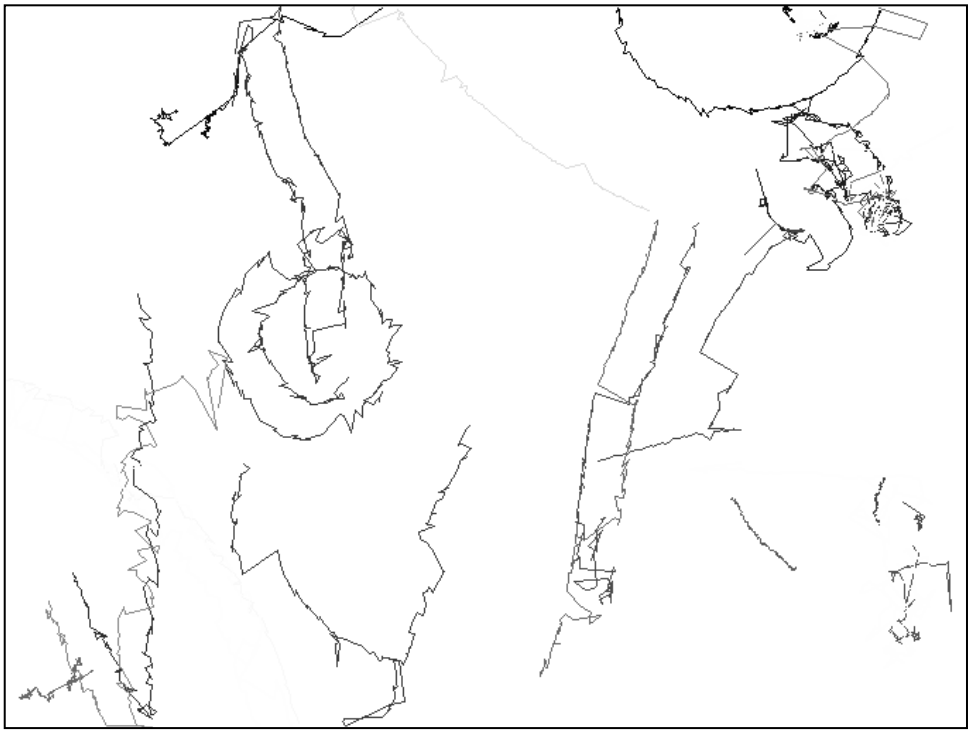

Figure 31. UU2768 413G, 1 µM serine added, top of slide with tracked paths

UU2768 413V

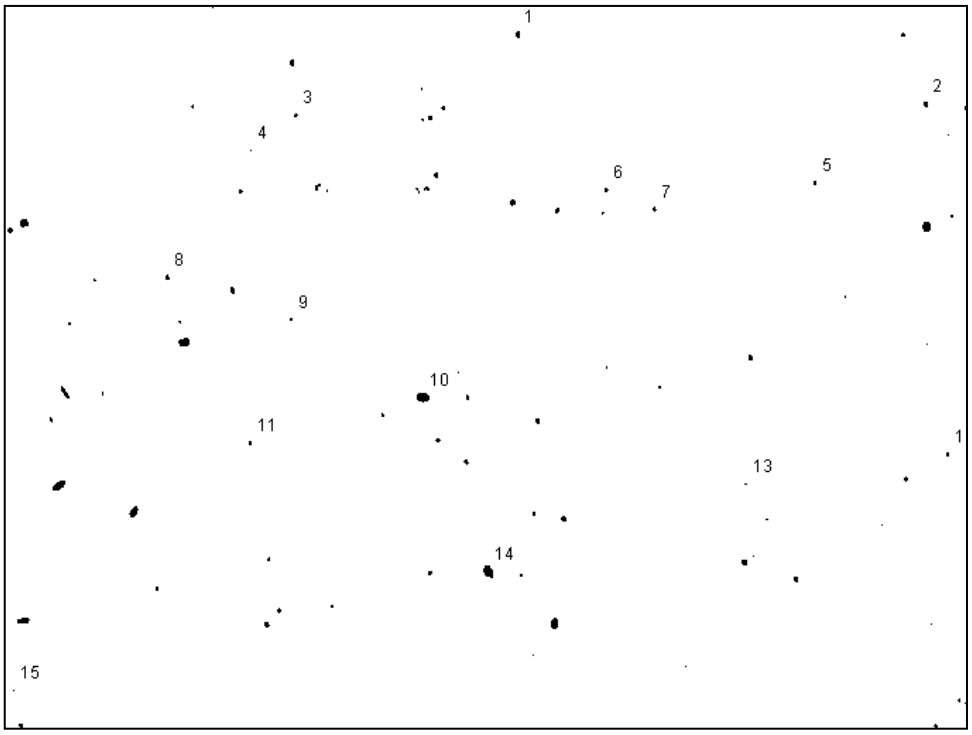

Figure 32. UU2768 413V, no serine added, bottom of slide with numbered labels

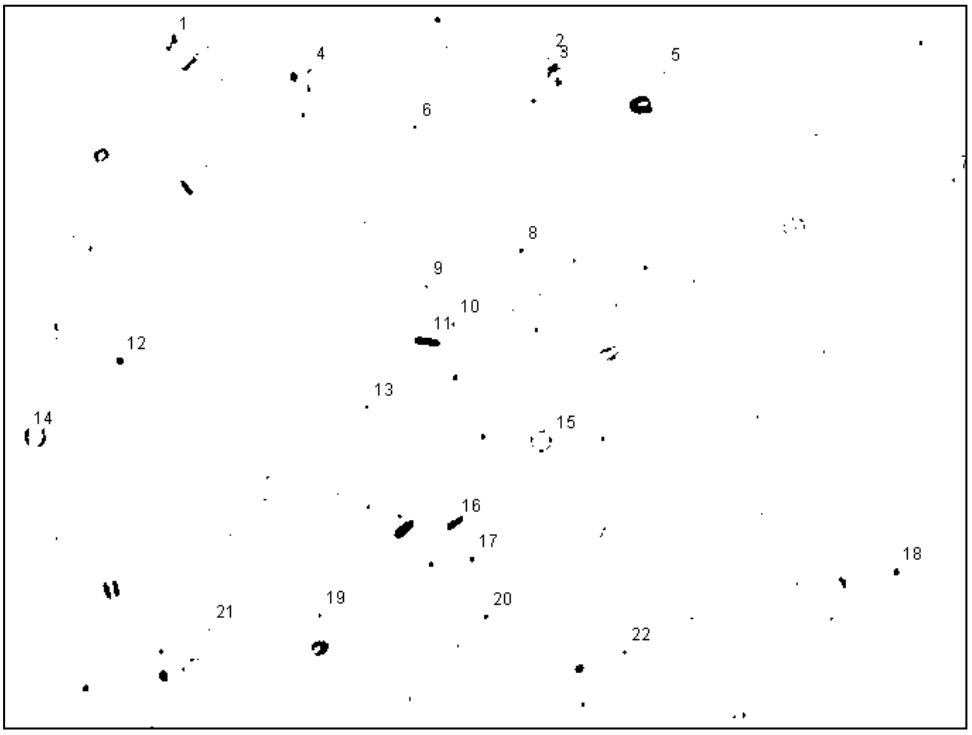

Figure 33. UU2768 413V, no serine added, top of slide with numbered labels

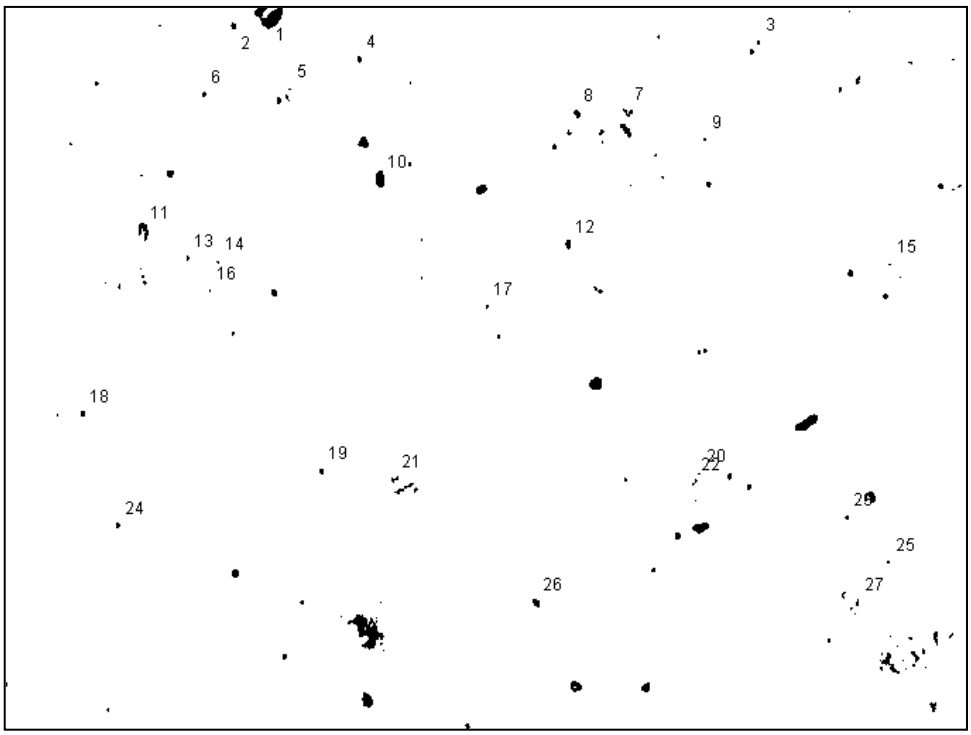

Figure 34. UU2768 413V, 1 µM serine added, bottom of slide with numbered labels

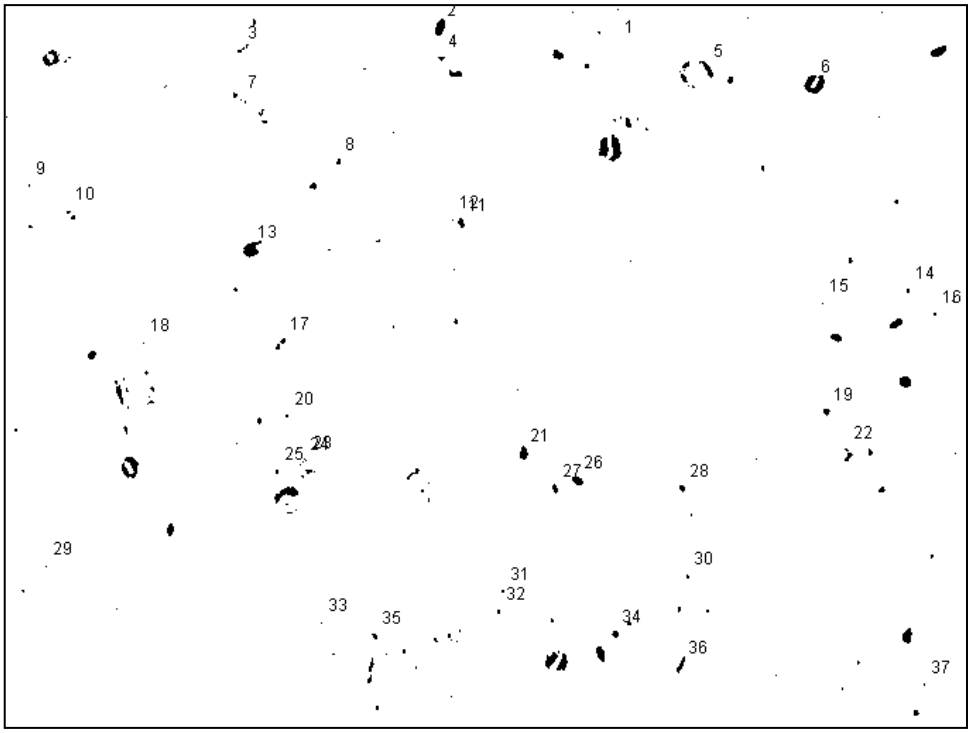

Figure 35. UU2768 413V, 1 µM serine added, top of slide with numbered labels

Figure 36. UU2768 413V, no serine added, bottom of slide with tracked paths

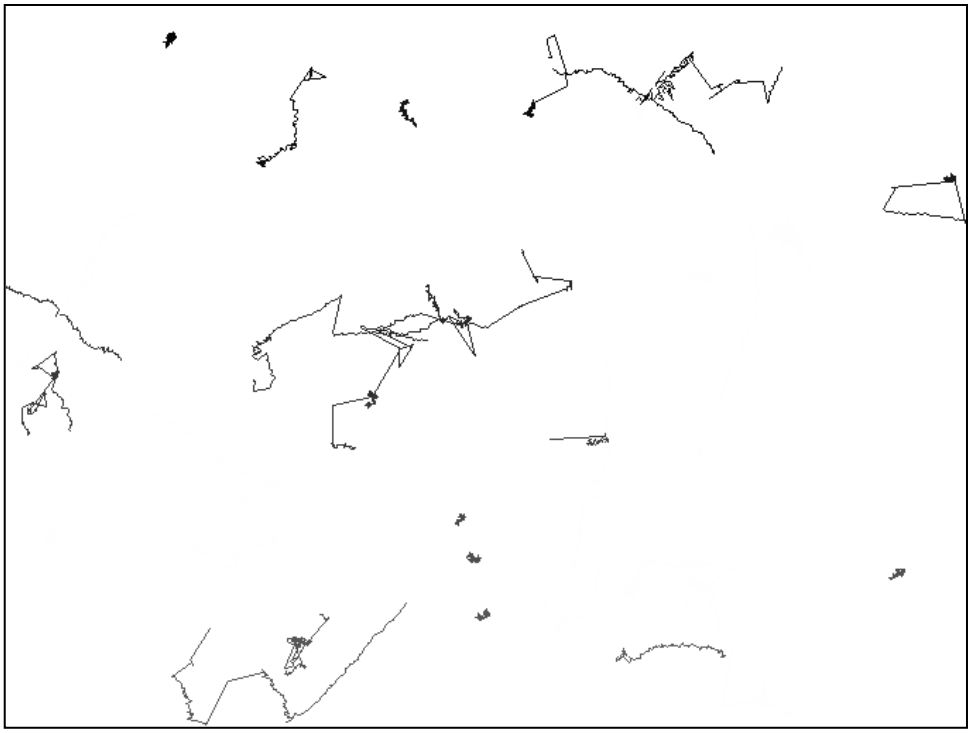

Figure 37. UU2768 413V, no serine added, top of slide with tracked paths

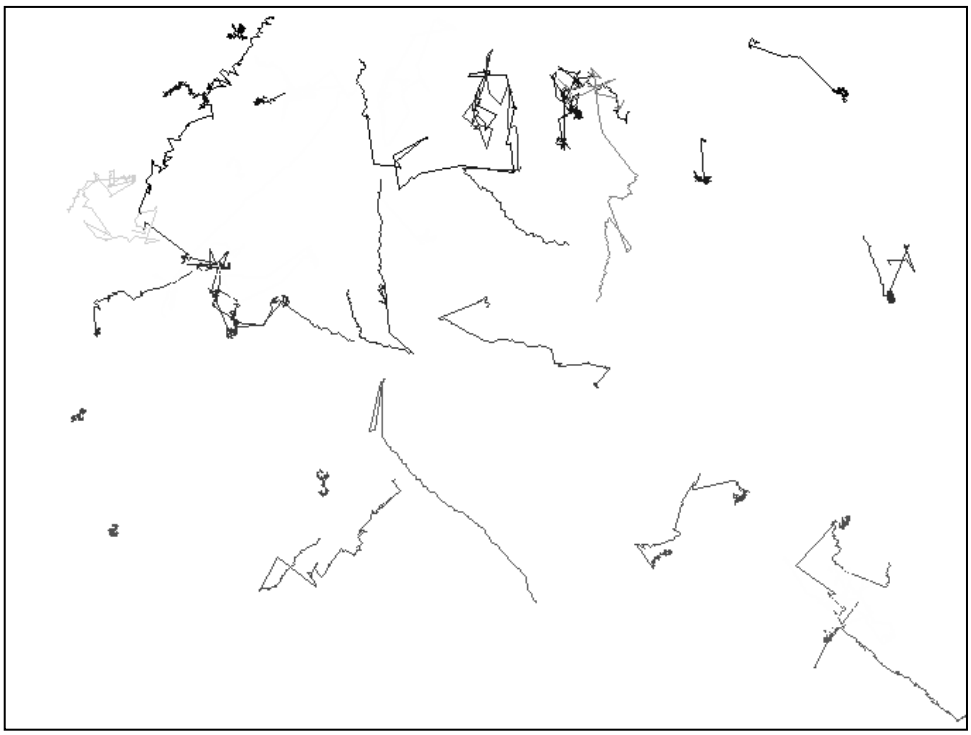

Figure 38. UU2768 413V, 1 µM serine added, bottom of slide with tracked paths

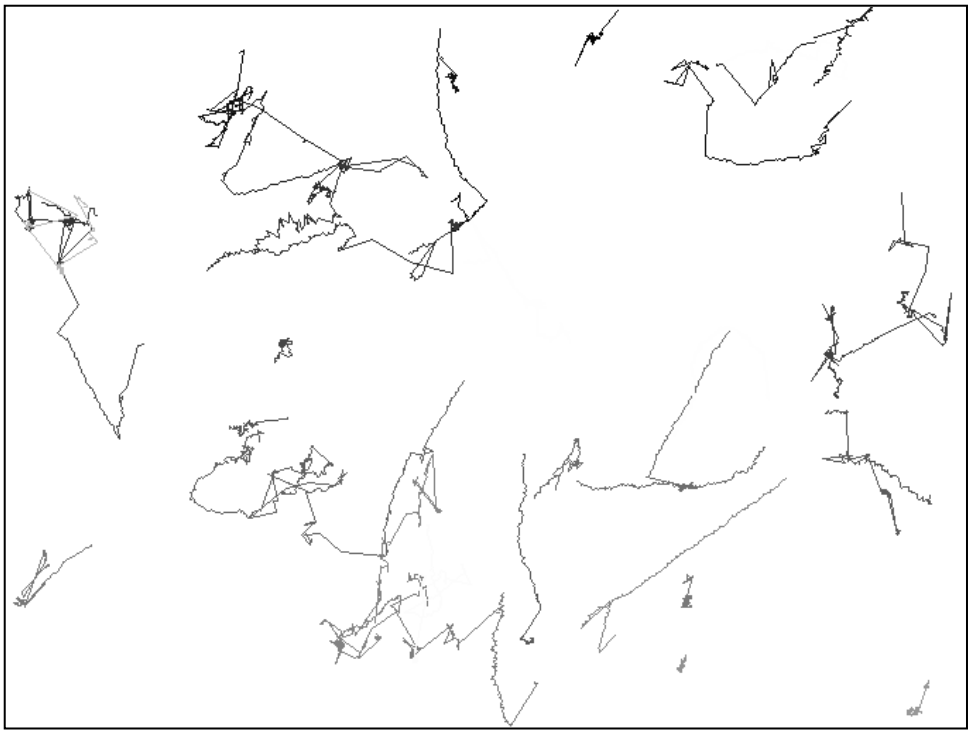

Figure 39. UU2768 413V, 1 µM serine added, top of slide with tracked paths

CHAPTER IV

CONCLUSION

The normal motility response for A413V cells in *E. coli* should result in a kinase-off signaling state with smooth swimming and counterclockwise behavior while the A413G mutation when observed has constant tumbling behavior. Comparing the known motions of *E. coli* to UU2766 A413G, UU2768 A413G, UU2766 A413V, and UU2768 A413V bacteria samples, UU2766 A413G followed consistently with constant tumbling with and without serine added to the sample. UU2766 A413V began tumbling and switched to smooth swimming after adding serine indicating that serine was effective when switching the kinase mechanism for this particular mutated strain. UU2768 A413G produced inconclusive data to be able to indicate whether or not serine was effective in switching the kinase mechanism. UU2768 A413V though initially began a mixture of swimming and mild tumbling after introducing serine to the cells tumbling increased tremendously which is consistent to A413V *E. coli* cells. Future studies to be done in a similar fashion for observing chemotactic behavioral response include the addition of IPTG, Serine, DMF, and Indole or the lack there of. Other variables to be changed are the deletion of CheB or expressing it in the cell which affects the adaption response of the cells to any stimuli. Observing the sample whether it begins swimming and transition to tumbling or vice versa. Including Tsr or deleting tsr which is the serine sensing chemoreceptor. Lastly, observing whether the cells respond to an attractant or repellant when introduced in the sample. In the attractant, the cells would swim toward the concentration gradient while in the repellant the cell's behavior should respond in swimming away from the concentration gradient.

REFERENCES

1. Hazelbauer GL, Falke JJ, & Parkinson JS (2008) Bacterial chemoreceptors: high-performance signaling in networked arrays. *Trends Biochem Sci* 33:9-19.

2. Zhou Q, Ames P, and Parkinson JS (2009) Mutational analyses of HAMP helices suggest a dynamic bundle model of input-output signalling in chemoreceptors. *Mol Microbiol* 73:801–814.

3. Zhou Q, Ames P, and Parkinson JS (2011) Biphasic control logic of HAMP domain signalling in the *Escherichia coli* serine chemoreceptor. *Mol Microbiol* 80:596–611.

4. Turner L, Ryu WS, and Berg HC (2000) Real-time imaging of fluorescent flagellar filaments. *J Bacteriol* 182:2793–2801.

5. Liu J, *et al.* (2012) Molecular architecture of chemoreceptor arrays revealed by cryoelectron tomography of *Escherichia coli* minicells. *Proc Natl Acad Sci USA* 109:1481–1488.

6. Briegel A, *et al.* (2013) The motility of two kinase domains in the *Escherichia coli* chemoreceptor array varies with signaling state. *Mol Microbiol* 89:831–841.